Pergamon

Cement and Concrete Research 31 (2001) 13–17

CEMENT AND CONCRETE RESEARCH

An XRPD profile fitting investigation of the solid solution between ettringite, $Ca_6Al_2(SO_4)_3(OH)_{12}\cdot 26H_2O$, and carbonate ettringite, $Ca_6Al_2(CO_3)_3(OH)_{12}\cdot 26H_2O$

S.J. Barnett[1], C.D. Adam*, A.R.W. Jackson

School of Sciences, Staffordshire University, College Road, Stoke-on-Trent, Staffordshire, ST4 2DE, UK

Received 16 March 1999; accepted 11 September 2000

Abstract

The solid solution between ettringite ($Ca_6Al_2(SO_4)_3(OH)_{12}\cdot 26H_2O$) and carbonate ettringite ($Ca_6Al_2(CO_3)_3(OH)_{12}\cdot 26H_2O$) has been investigated by X-ray powder diffraction (XRPD) full pattern fitting. A single solid-solution phase was found when SO_4^{2-} was the majority anion, while two phases existed when CO_3^{2-} predominated. It is proposed that the formation of two phases is due to a crystallographic incompatibility between the two end members and hence, no mechanism for a continuous solid-solution series from one to the other is possible. Interpreting the data using the variation in unit cell volume as a function of chemical composition and through a unit cell parameter map, a more detailed examination of the crystallography of the phases was possible. This showed that the solid-solution mechanisms at the atomic level lead to complex yet consistent changes in the unit cell shape and volume that are readily followed by modern powder diffraction methods.

Keywords: Ettringite; Solid solutions; X-ray diffraction

1. Introduction

Ettringite ($Ca_6Al_2(SO_4)_3(OH)_{12}\cdot 26H_2O$) and its carbonate analogue ($Ca_6Al_2(CO_3)_3(OH)_{12}\cdot 26H_2O$) are of considerable interest in cement applications [1–3]. These phases have previously been synthesised and characterised by X-ray diffraction [4] and the solid solution between them has been investigated [5]. This paper describes part of a project [6,7] in which modern methods of X-ray powder diffraction (XRPD) data analysis, such as full pattern fitting [8] and Rietveld refinement [8,9], are being evaluated as a means of identifying the exact nature of ettringite, thaumasite and other related phases, as well as their solid solutions, in cementitious systems.

Full pattern fitting [8] is an XRPD data analysis technique, which uses the whole of the powder pattern to calculate accurate unit cell dimensions and intensities. It is a least-squares technique in which a calculated pattern is produced from a refinable model and fitted to the experimental data in an iterative procedure. The refinable model includes information about the crystal class, Miller indices of reflections, approximate unit cell dimensions, instrumental and sample-dependent effects. No information on the types or positions of the atoms present in the crystal structure is required or obtained. Refined values of relative intensities, cell parameters, 2θ corrections and peak profile coefficients are produced. This technique is now capable of refining these parameters for several phases in a mixture simultaneously; meaning that it can now be applied to cement systems. For example, Gutteridge [10] used a similar but less flexible technique to quantify real Portland cement systems by fitting to standard patterns for the phases present. The fitting technique used in this present work has been shown to produce unit cell dimensions in multiphase systems to a high degree of accuracy (± 0.008 to ± 0.015 Å), even when there is significant peak overlap [6]. These error bars have been verified through extensive work on pure phases in mixtures, using accepted internal standards, and include the end members of the solid-solution series being studied here.

* Corresponding author. Tel.: +44-1782-294679; fax: +44-1782-745506.

E-mail address: c.d.adam@staffs.ac.uk (C.D. Adam).

[1] Present address: Department of Chemistry, University of Aberdeen, Meston Walk, Aberdeen, AB24 3UE, UK.

0008-8846/01/$ – see front matter
PII: S0008-8846(00)00429-4

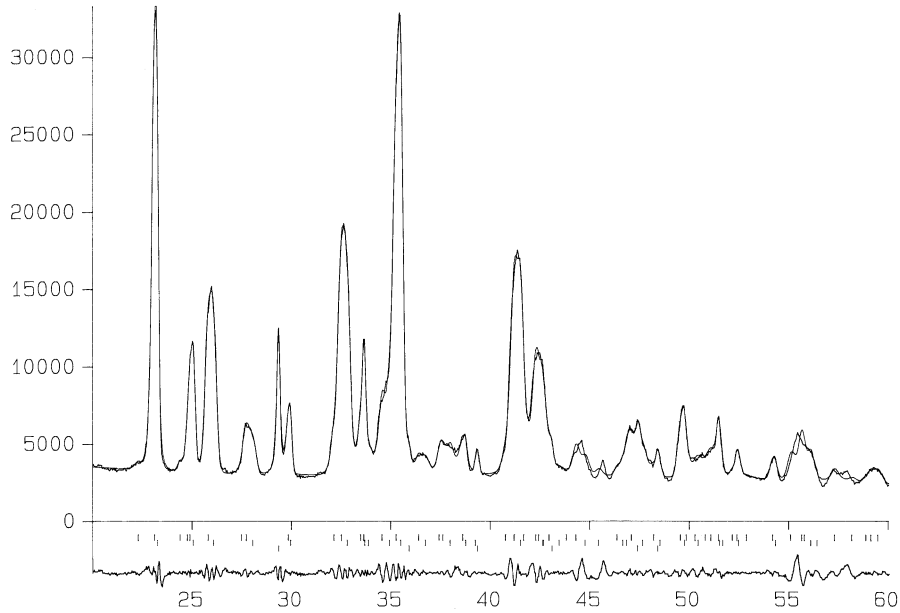

Fig. 1. The profile fitted XRPD pattern for the 40% SO_4^{2-} preparation; both the experimental data and least-squares fitted profile are shown together with the difference function. Peak positions are indicated just below the 2θ axis; the uppermost line corresponding to the ettringite-based solid solution, the next the carbonate ettringite-based solid solution, and the lowest line a trace of calcite.

The work presented here concerns the application of this technique to the solid solution between ettringite and its carbonate analogue, which was previously investigated by Pöllmann et al. [5].

2. Experimental

Eleven members of the solid-solution series between ettringite and carbonate ettringite were synthesised under CO_2-free conditions. Each member of the series was prepared by mixing a slurry of calcium oxide in sucrose solution with one of sodium aluminate plus varying amounts of sodium sulphate and sodium carbonate. All water used was freshly boiled distilled water and the calcium oxide was baked overnight at 950°C to remove any calcium carbonate present. In each case, the solid produced was isolated by suction filtration, washed with distilled water followed by acetone, and dried at room temperature, in CO_2-free conditions. Chemical analysis of the solids confirmed the SO_4^{2-} level was consistent with that in the preparation as a whole. Rietveld refinement [6] of the XRPD pattern from the 50% SO_4^{2-} sample confirmed the SO_4^{2-}:CO_3^{2-} ratio.

XRPD data was collected for each member of the series using a Philips PW1050 diffractometer with CuKα radiation, driven by a Hiltonbrooks control system. Data was collected over the 5–75° 2θ range, using a step size of 0.04° and a count time of 20 s per step. Full pattern fitting was carried out using the BESTFIT program developed by Adam [11], with the ICDD standard patterns for synthetic ettringite and carbonate ettringite [12] used to provide initial approximate unit cell dimensions and Miller indices for the fitting process. The 20–60° section of the pattern was used consistently for this analysis. An example of a profile fitted experimental XRPD pattern is given in Fig. 1. The goodness of fit is demonstrated by the difference plot shown at the foot of this figure.

3. Results

Either one or two ettringite-type phases were produced in all preparations. Calcite ($CaCO_3$) was identified as a very minor impurity in several samples. The composition of each sample is expressed as the mole percent of each anion (SO_4^{2-} or CO_3^{2-}) as a proportion of the total anion moles present. Trends in the behaviour of the unit cell parameters, obtained for the solid-solution series by full pattern fitting,

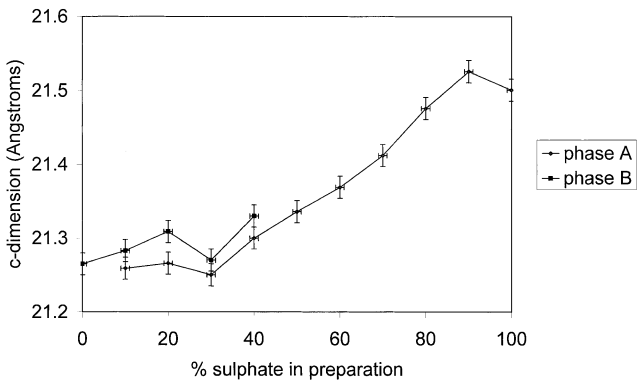

Fig. 2. Unit cell *c*-axis as a function of % SO_4^{2-} in the preparation.

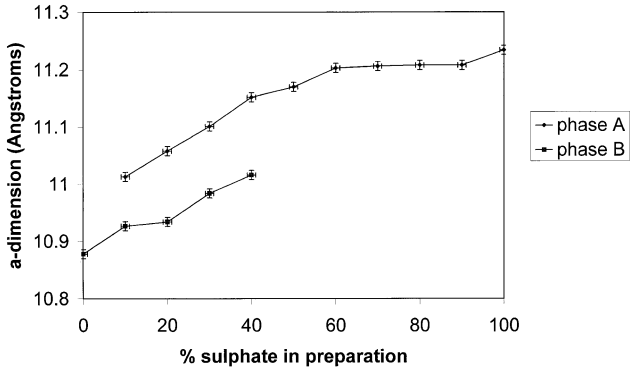

Fig. 3. Unit cell *a*-axis as a function of % SO_4^{2-} in the preparation.

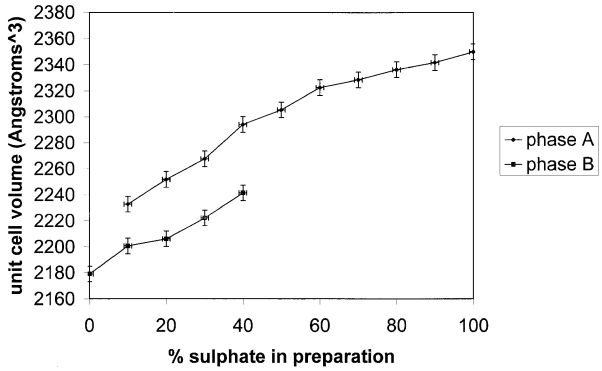

Fig. 5. Unit cell volume as a function of % SO_4^{2-} in the preparation.

are illustrated in the following graphs: The following graphs illustrate the changes in each of the unit cell dimensions as a function of chemical composition:

- The variation in the unit cell *c*-dimension as a function of composition,
- The variation in the unit cell *a*-dimension as a function of composition,
- A unit cell "map" of the *c*-dimension vs. the *a*-dimension,
- A graph of unit cell volume vs. composition.

These are shown graphically in Figs. 2–5.

The *c*-axis (Fig. 2) behaves as previously reported [5] except that this present work shows more clearly that, at low SO_4^{2-}, the second phase (termed here the B phase) is not necessarily pure carbonate ettringite but apparently a second solid solution. This conclusion is supported by the clear trend in the *a*-axis dimension (Fig. 3), which is fairly constant from 100% to 60% SO_4^{2-} thereafter dropping steadily. The two phases (A and B) both show fairly similar reductions in the *a*-axis towards low SO_4^{2-} levels but quite different absolute values. The *a*-axis of the B phase is not constant at low % SO_4^{2-}.

The unit cell parameter map (Fig. 4) allows examination of the unit cell, independent of the composition co-ordinate. The plot shows three regions with different characteristics.

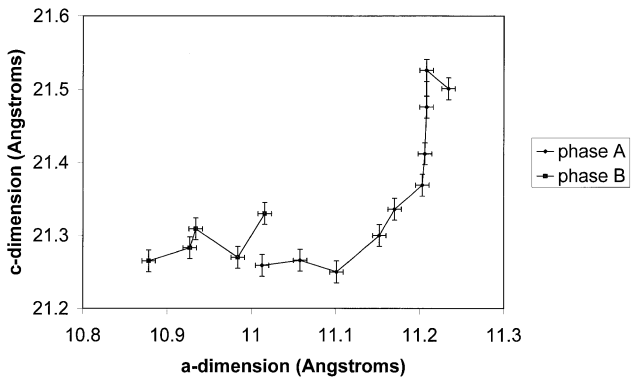

Fig. 4. Unit cell parameter map.

The high SO_4^{2-} end from 100% to 60% where, after an initial small rise, the *c*-axis falls rapidly with little accompanying change to the *a*-axis. From 60% to 30% SO_4^{2-}, both cell parameters decrease uniformly. At the low SO_4^{2-} end where both A and B phases exist, the trends show similarities and differences. There is a rapid decrease in the *a*-axis for both phases. The *c*-axis of the A phase remains fairly constant while that of the B phase appears to show little evident correlation though converging towards the carbonate-ettringite end member.

The unit cell volume ($V = a^2 c \sin\gamma$) (Fig. 5) shows very clear smooth behaviour with changing composition. For phase A, there appear to be two linear sections each occupying half the composition range. The high SO_4^{2-} half shows a low gradient (slope = 0.68) while the lower SO_4^{2-} half has a higher gradient (slope = 1.87). The cell volumes for phase B show a trend with composition, which is at a similar rate to phase A but displaced to lower volumes. Note that the end member (carbonate ettringite) actually lies on the phase B trend line.

None of the XRPD patterns showed evidence of any amorphous material. The pattern fitting approach used in this data analysis is particularly powerful in determining whether the experimental pattern shows any deviation from a model comprising a simple mixture of crystalline phases. We have found an amorphous phase in other preparations of similar materials not directly connected with this work [6].

4. Discussion

These results show that XRPD, coupled with full profile fitting techniques, is a powerful tool in elucidating the subtle crystallographic changes within solid-solution phases. The high quality of these measurements is founded upon the relatively small error bars on *a* and *c* arising from the fitting technique, supported by the clear trends shown in many of the unit cell plots, especially that shown for unit cell volume as a function of the mixture composition.

As in the original study [5] of this solid-solution series, this present work identified two ettringite-type phases present at higher carbonate contents with only one at the

high sulphate end. Inspection of the variation of unit cell volume against composition (Fig. 5) provides a monitor of the overall changes within the structure. There appear to be two distinct rates of change depending on whether SO_4^{2-} or CO_3^{2-} is the majority anion. In the case where the former is the dominant anion, replacement of the larger SO_4^{2-} by the smaller CO_3^{2-} has less effect on the overall cell volume so the rate of contraction is low. In the case where CO_3^{2-} is dominant, substitution by the larger SO_4^{2-} has the effect of changing the magnitude of the cell volume more rapidly. In both cases, the structural influence of the larger anion appears to dominate. Both the phases present at low SO_4^{2-} concentrations (phases A and B) show very similar rates of change in cell volume. Hence, we can conclude that since there is a smooth transition from the carbonate-ettringite end member to the phase B trend line, phase B is clearly a solid solution based on the carbonate-ettringite structure. Conversely, phase A is based on the sulphate-ettringite structure, though the different rates of change of the cell volume above and below 50% SO_4^{2-} suggest that two variants of this structure are present in these samples. It is clear from this data that there is no continuity of crystal structure across the solid-solution series. At intermediate anion compositions, either or both of phases A and B can exist but they remain crystallographically distinct.

Looking at the unit cell map (Fig. 4) allows a more detailed examination of the changes occurring within the unit cell. For phase A, there are clearly three distinct regions of behaviour which occupy approximately equal ranges of composition. Since the ettringite structure contains three distinct anion sites (symmetry yields a second pairing site for each), it is feasible that there is some systematic way in which these sites are occupied within this solid-solution series. Indeed, more recent work [13] using Rietveld refinement to determine the crystal structure of carbonate ettringite indicates that anion sites, as measured by the distances between the anions along the channels, vary in size. This has also been found previously in the structure of sulphate ettringite, though to a lesser extent [14]. The implication of this is that there would be preferential anion exchange to sites where a lower level of lattice distortion would result. Such a mechanism would control the progress of the solid-solution series across the composition range and indeed could explain the observed expansion of the *c*-axis on incorporation of very small proportions of CO_3^{2-} (Fig. 2). In any case, these results indicate that the changes in the crystal structure across the series are quite complex, though systematic, and are consistent with a smooth change in unit cell volume.

Examination of this plot shows further interesting features where carbonate is the majority anion. In those samples where this occurs, both phases A and B exist. Phase A maintains the cell aspect ratio (i.e. *c*/*a*) as the SO_4^{2-} concentration decreases from 60% to 30%, which compresses its *c*-axis to just less than that of the carbonate end member. The *a*-axis then contracts significantly but in the 10% SO_4^{2-} sample it remains well away from that of the carbonate end member. This behaviour suggests that this phase (A) can incorporate significant CO_3^{2-} within a SO_4^{2-}-ettringite structure but in this last sample, has reached its maximum capacity. The assumption that the cell volume is a linear measure of the SO_4^{2-}:CO_3^{2-} ratio may be tested. On this basis, these results imply that the unit cell volume of this terminal A phase occupies a position 68% away from the sulphate ettringite and 32% from the carbonate-ettringite end members. This apparent replacement of two-thirds of the sulphate by carbonate is what was proposed in the previous study on these systems [5]. The cell volume plot, which shows that extrapolation of the phase B line leads to the sulphate-ettringite end member, appears to support this simple proportional relationship between composition and unit cell volume. However, the implication of this for phase A is that, between 0% and 50% SO_4^{2-}, the anion composition in the solid phase does not equal that in the preparation. This also leads to inconsistencies in the total SO_4^{2-} content apportioned between the two phases at the opposite end of the solid-solution series. It is concluded that the link between unit cell volume and composition is more complex than this supposition suggests.

The unit cell map (Fig. 4) also shows interesting indications as to the formation of the two phase systems. Phase A formed in the 10% SO_4^{2-} mix appears to terminate that phase. The *c*-axis corresponds approximately to that in the carbonate ettringite but the *a*-axis is significantly larger than that of the end member. It appears that it is impossible for this structure to lose the last few percent of SO_4^{2-} and transform into the carbonate end member as it is crystallographically incompatible with that structure. Phase B is formed below 50% SO_4^{2-} by a sudden decrease in the *a*-axis (to the same value which phase A has at 10% SO_4^{2-}) with no change in the *c*-axis. By this means, it transforms crystallographically to a structure, which can converge through a series of iterative-like changes in cell dimensions, to the carbonate-ettringite end member.

The question of the exact chemical composition of these solid-solution phases remains unresolved. This XRPD study has, however, shown how they may be crystallographically characterised to a high degree of precision.

The chemical composition of these solid-solution phases was not determined as techniques are not readily available which will reliably measure the elemental composition within the individual crystalline components. Given that the exact chemical composition of these crystalline phases is unknown, it is possible that at low SO_4^{2-} concentrations in the mixture, phase B is actually the carbonate-ettringite end member. This proposition has been tested by attempting pattern fitting of the XRPD patterns of these mixtures, with the unit cell parameters of phase B fixed at those of carbonate ettringite. These attempts failed to produce an adequate fit of observed and calculated data since the positions of the reflections due to carbonate ettringite did

not correspond to the positions of the reflections of either of the ettringite-type phases present in the samples. Therefore, it is possible to conclude that phase B is not simply the carbonate end member.

We have already stated that there is little or no amorphous material present. Despite the lack of chemical analytical data, there are strong indications that the SO_4^{2-}:CO_3^{2-} ratios within the preparations here are a fairly accurate reflection of the composition of the crystalline phases produced. Although some calcite was observed in most samples, this was consistently found as a very minor component at the few percent level. A separate study [6] where Rietveld refinement of synchrotron X-ray data obtained from the 50% SO_4^{2-} sample was carried out, found that the SO_4^{2-}:CO_3^{2-} ratio, within the single crystalline phase, was 54:46, with an error bar of ±3.

5. Conclusions

This study of the solid-solution series between ettringite and its carbonate analogue has shown further evidence of fascinating crystallographic features within these systems and the power of XRPD profile fitting as an investigative tool.

The XRPD evidence suggests that there is no smooth transition across the solid-solution series but rather two distinct solid-solution structures (referred to as A and B in this work) based on the two end members. Within each of these structures, there are smooth crystallographic changes, shown by the unit cell volume, consistent with changes in chemical composition. The rate of expansion or contraction of this volume occurs in linear sections, which it is proposed is a result of whether SO_4^{2-} or CO_3^{2-} is the majority anion. The unit cell map shows more detailed information on the mechanisms of these crystallographic changes indicating systematic behaviour in the cell dimensions, which relates to the active anion exchange sites within the structure. Further work is needed to link these subtle changes to the occupancy and orientation of the anions and water molecules within the channels and the mechanisms by which they affect the structural periodicity of the columns within the ettringite structure.

Acknowledgments

The authors would like to thank Dr. P.D. Hywel-Evans for his advice. We are grateful to Fosroc International for their collaboration and financial support.

References

[1] E. Henderson, X. Turrillas, P. Barnes, The formation, stability and microstructure of calcium sulphoaluminate hydrates present in hydrated cement pastes using in-situ synchrotron energy-dispersive diffraction, J. Mater. Sci. 30 (1995) 3856–3862.
[2] S.A. Brookes, J.H. Sharp, in: R.J. Mangabhi (Ed.), Calcium Aluminate Cements, Chapman & Hall, London, 1990, pp. 335–347.
[3] M.N. Muhamad, P. Barnes, C.H. Fentiman, D. Hausermann, H. Pollmann, S. Rashid, A time-resolved synchrotron energy-dispersive diffraction study of the dynamic aspects of the synthesis of ettringite during minepacking, Cem. Concr. Res. 23 (1993) 267–272.
[4] L.J. Struble, Synthesis and characterisation of ettringite and related phases, 8th Int. Congr. Chem. Cem. Rio, vol. VI (1987) 582–588.
[5] H. Pöllmann, H.-J. Kuzel, R. Wenda, Solid solution of ettringites: 1. Incorporation of OH^- and CO_3^{2-} in $3CaO{\cdot}Al_2O_3{\cdot}3CaSO_4{\cdot}32H_2O$, Cem. Concr. Res. 20 (6) (1990) 941–947.
[6] S.J. Barnett, X-ray powder diffraction studies of ettringite and related phases. PhD Thesis, Staffordshire University, UK (1998).
[7] S.J. Barnett, C.D. Adam, A.R.W. Jackson, P.D. Hywel-Evans, Identification and characterisation of thaumasite by XRPD techniques, Cem. Concr. Compos. 21 (1999) 123–128.
[8] J.I. Langford, D. Loüer, Powder diffraction, Rep. Prog. Phys. 59 (1996) 131–234.
[9] R.A. Young (Ed.), The Rietveld Method, Oxford Univ. Press, UK, 1993.
[10] W.A. Gutteridge, Quantitative X-ray powder diffraction in the study of some cementive materials, Proc. Br. Ceram. Soc. 35 (1984) 11–23.
[11] C.D. Adam, IUCr Powder Diffraction Symposium, Toulouse, France, IUC, UK, 1990. 269 pp.
[12] ICDD Powder Diffraction File, 1989, Card Numbers 37-1476, 36-1465.
[13] S.J. Barnett, C.D. Adam, A.W.R. Jackson, Rietveld refinement of ettringite, thaumasite and related phases, in preparation.
[14] A.E. Moore, H.F.W. Taylor, Acta Crystallogr. Sect. B 26 (1970) 386–393.